University of Utah
UNDERGRADUATE RESEARCH JOURNAL

JOINT DISTANCE, COVERAGE AND CONGRUENCY ANALYSIS OF THE TIBIOTALAR JOINT

Andrew Peterson (Amy L. Lenz, PhD)
Department of Biomedical Engineering and Department of Orthopaedics

INTRODUCTION: Historically, our morphometric understanding of the ankle joint complex has been derived primarily from 2D measurements of conventional radiographs. The advent of volumetric imaging, including CT and MRI has made it possible to generate 3D reconstructions of the bones of the ankle joint complex [1]. Weightbearing CT scans provide an added benefit to assess pathology such as malalignment, impingement, and joint space narrowing that may be overlooked in the absence of physiological loading. Specifically, improving the 3D morphological relationship definitions of the tibia and talus in the tibiotalar (TT) joint allows for a better understanding of pathological patterns and outliers. A computational morphometrics technique termed statistical shape modeling (SSM) can be used to visualize and analyze morphological differences in 3D and enables the identification of mean bone shapes and shape modes of variation using correspondence particles (mathematically placed points of interest throughout the bone's surface). We previously applied SSM to study variations in the anatomy of the tibia and talus; however, joint coverage, distance and congruency were not evaluated with these morphological differences in mind. There are a few studies that have measured TT joint distance in weightbearing CTs and reported findings in six to nine average regions within the articulating surface [2,3]. Joint congruency has been investigated previously in other joints, such as the thumb carpometacarpal joint [4], but to our knowledge congruency has not been analyzed throughout the TT joint. Congruency, joint distance and coverage may change with the onset of osteoarthritis (OA). Two-dimensional weight-bearing radiographs are still the clinical standard for diagnosing diseased ankles presenting with OA, chronical ankle instability and/or hindfoot deformity. However, with the advent of high-resolution weightbearing CT imaging techniques, 3D metrics to quantify the TT joint are necessary to improve treatment planning and longitudinal tracking of patients' ankle health. For example, the ability to quantify joint distance, coverage and congruency merged with the bone morphology variances could provide clinicians with tools to assist in diagnosis and pre-operative planning for patients with ankle diseases. The objective of this study was to quantify TT joint distance, coverage, and congruency for healthy individuals using weightbearing computed tomography (CT) images and SSMs.

METHODS: Twenty-seven asymptomatic controls (age: 50.0 ± 7.3 years; height: 169.4 ± 6.4 cm; BMI: 25.3 ± 3.8 kg/m2; 7 males) previously underwent weight-bearing CT scans (Planmed Verity; 0.4 x 0.4 x 0.4 mm voxels) with IRB approval. Participants were aligned in the CT scanner such that the vector between the calcaneus and second metatarsal were positioned relative to the scanner's anterior-posterior axis. For each participant, CT images were segmented to create 3D models of the tibia and talus (Amira, v6.0.1, Visage Imaging). Using the 2nd principle of curvature and a joint coverage calculation in PostView (v2.1.0, FEBio Software Suite, University of Utah), the articulating surface on the talar dome and tibial plafond were isolated. The isolated articular surface areas in the coverage region were defined as the mathematical region where the surfaces contained intersecting normal vectors. A paired t-test compared the surface area of the articulating region of the tibia and talus. The surface mesh within the identified coverage regions was used to calculate joint distance, mean curvatures and Gaussian curvatures for all participants using PostView. A previously completed SSM mean talar shape was mathematically aligned and compared to each participant's talus to determine common correspondence particle locations across all participants [5]. Joint distance and congruency were calculated at each common correspondence particle using MATLAB (R2017b, MathWorks, Natick, MA, USA). The congruency index, a measure to quantify the matched articular surfaces, was calculated based on methods described by Ateshian et al [4]. The congruency index scale begins at 0 mm^{-1}, which defines perfectly congruent surfaces. Joint distance and congruency index values were averaged across the studied population at common correspondence particle locations.

RESULTS: In our healthy population during a weight-bearing position, the TT articulating surfaces yielded a significantly greater tibial surface area (943.2 ± 103.6 mm^2) when compared to the talar surface area (791.9 ± 83.4 mm^2) ($p < 0.05$). The TT joint distance was uneven with a larger posterior lateral distance (~3 mm) that slightly narrowed in the anteromedial region (~2 mm) and was even narrower in the anterolateral region (~1 mm) (Figure 1). Across the healthy population, participants had an average TT joint distance of 2.1 ± 0.4 mm (range: 1.1 – 3.5 mm). The TT joint articulating surface was evenly congruent throughout with an average congruence index of 0.15 ± 0.07 mm^{-1} (range: 0.06 – 0.38 mm^{-1}) and slight variation around the perimeter of the anterior articulating region (Figure 1). The joint distance and congruence index for each participant was consistent with the reported mean trends (see a representative individual in Figure 2).

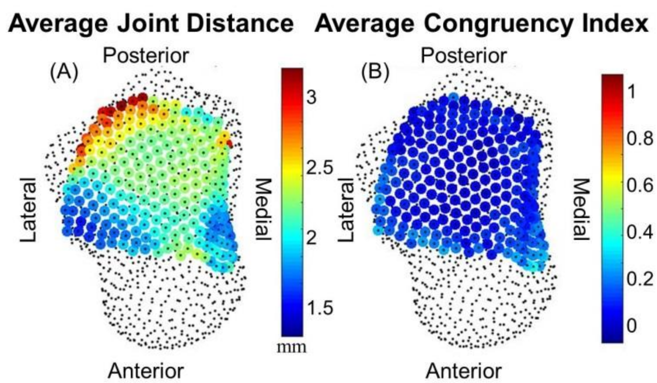

Figure 1: Mean shape of talus with data mapped to the correspondence particles with joint distance values (A) and congruency indices (B) found at each particle. On average, distance was greater in the posterior region while congruency varied little throughout the surface.

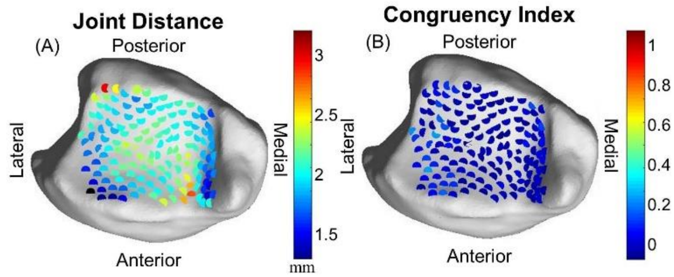

Figure 2: A representative participant's joint distance (A) and congruency indices (B). There are variations in the joint distance, but little to no change in the congruency throughout the articulating space.

DISCUSSION: Our study reported that despite individual participant bone morphology variations, trends across individual participants remained consistent for joint distance, tibial coverage surface area, and the congruency index profile. In our SSM models, we have observed talar and tibial bone shape variation including: the width of the talar trochlea and curvature in the inferior articulating surface and tibial plafond rate of curvature variations (Figure 3), yet despite these morphological differences, congruency remains consistent in this healthy population. These findings highlight the necessity to consider anatomical variations in the shape of the talus and tibia as independent bones along with analysis of the interaction of these two bones as a joint when evaluating a patient's joint health, alignment and function. When the joint has varying morphological structures in healthy individuals, but is congruent throughout, a better understanding of the articular joint relationship is gained. The results presented can serve as an initial control data set to establish 3D TT joint metrics that can be used for a comparison with pathological populations. Additionally, the results can provide baseline morphometrics to consider when designing future total ankle replacement prostheses. Future research should apply the developed quantitative 3D metrics to dynamic in-vivo assessment of the TT joint. For example, it could be clinically important to understand the effects of talar trochlea rates of curvature on joint distance and congruency throughout the joint's full range of motion. A better understanding of the congruency of the TT joint during functional activities could provide additional biomechanical insight to the role the joint plays in the development of OA and other ankle diseases. Further studies should analyze how bone morphology affects joint distance and congruency in patients with OA. Ideally, the combination of high-resolutions volumetric imaging and 3D morphometrics could be used to improve the treatment of patients suffering from OA and other diseases in the ankle joint complex. These tools will hopefully provide better 3D metrics for clinicians to link joint morphology findings to individual bone variability as observed on weightbearing CT scans.

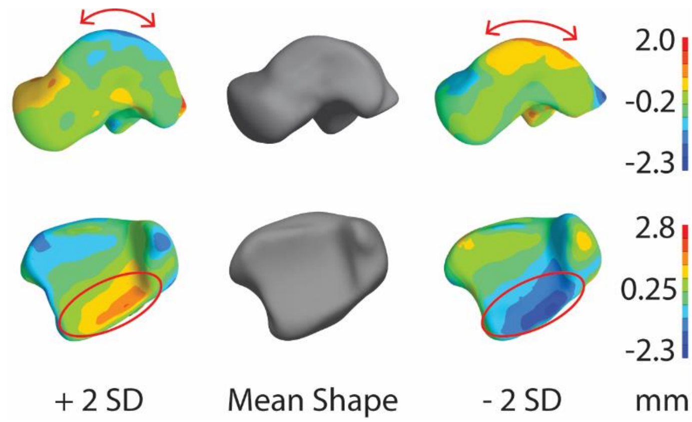

Figure 3: Talar and tibial mean shape with ± 2 standard deviations (SD) represented for a primary mode of variation, highlighting articular surface morphology variations across the population.

ACKNOWLEDGEMENTS: Funding was provided by the National Institutes of Health (R21AR069773, R01EB016701), Stryker/ORS Women's Research Fellowship, and the L.S. Peery Discovery Program in Musculoskeletal Restoration.

REFERENCES:

[1] Hayes, A et al., Iowa Orthop J., 26: 1-4, 2006.
[2] Siegler, S. et al., Journal of Biomechanics, 76: 204-211, 2018.
[3] Imai, K. et al., Journal of Foot and Ankle Research, 8:6, 2015.
[4] Ateshian, G. et al., Journal of Biomechanics, 25: 591-607, 1992.
[5] Lenz, A et al., Orthopaedic Research Society, 2019.